Quantum Waveguide Structures and Devices

S.M. Goodnick, A. Weisshaar, A. Ecker, and V.K. Tripathi
Department of Electrical and Computer Engineering
Oregon State University
Corvallis, OR 97331

Abstract

Nanometer structures in semiconductor heterojunction systems have been studied now for several years and have conclusively shown evidence for quantum interference phenomena and granular effects due to the finite number of electrons and impurities. Various proposals have been made for novel devices based on such effects which would serve as the basis for terabit memories and ultra-dense processing elements. Here a discussion is given of the application of a generalized mode matching scheme as a computational tool for investigating arbitrary quantum waveguide structures and discontinuities. Results are presented for the nonlinear conductance properties of multiple bend structures, lateral resonant tunnel structures, and nonequilibrium transport through quantum dot structures. Comparison is made to various experimental realizations of these structures where complications due to undesired inhomogeneities such as boundary roughness and impurities play a significant role.

1 Introduction

The theoretical transport properties of quantum waveguide structures with discontinuities have been modeled by a variety of different numerical methods. These include nearest-neighbor tight-binding schemes [1]-[3], mode-matching methods [4]-[7], and the finite element method [8]. In the present work, the modal analysis method based on the mode-matching technique is developed, and some of its typical characteristic properties are discussed. In the application of the modal analysis technique to quantum waveguides, the analogy to electromagnetic guided-wave structures is utilized. Convergence problems occurring with the mode-matching technique as applied to step discontinuities are discussed. Non-uniform quantum waveguide structures, which are composed of junctions and uniform waveguide sections, are analyzed by utilizing an extended generalized scattering matrix technique. The technique is applied here to study double-bend structures with right- angled and rounded corners. The calculated low-temperature conductance exhibits resonance peaks which compare to experimental measurements in split-gate AlGaAs/GaAs two-dimensional gas (2DEG) structures with bend discontinuities. The technique is further extended to transport through pinched quantum dot structures in which resonant tunneling occurs. A gate-controlled negative differential conductance is predicted much in analogy to the conventional double barrier structure.

2 Theoretical Model

The method presented here has been described in detail elsewhere [12]. It is assumed that the electronic motion inside the quantum waveguide is coherent (i.e. no inelastic scattering), and that the electronic states are governed by the time-independent Schrödinger equation in the effective mass approximation

$$\nabla^2\psi + \frac{2m^*}{\hbar^2}(E-V)\psi = \left(\nabla^2 + k_E^2 - k_V^2\right)\psi = 0 \quad (1)$$

with arbitrary lateral potential confinement $V(x)$. In (1), E represents the total electron energy, and the effective mass m^* is assumed to be isotropic. For simplicity, the system is assumed to be completely confined in the vertical growth direction, with only the ground state occupied for quantization in this direction.

The general wave solution for this two-dimensional waveguide structure is given as a superposition of propagating and evanescent modes

$$\psi = \sum_n \left(a_n e^{i\beta_n z} + b_n e^{-i\beta_n z}\right)\phi_n(x) \quad (2)$$

with

$$\beta_n = \sqrt{k_E^2 - k_V^2 + \frac{d^2\phi}{\phi dx^2}} \quad (3)$$

0-8186-6715-X/94 $4.00

where the transverse eigenfunctions ϕ_n and the (complex) phase constants β_n depend on the lateral potential profile. Only the hard-wall case with infinite potential walls and zero potential between the walls is considered here, although the technique is easily extended to more complex lateral potential profiles [9]. For uniform hard-wall waveguides of width w, the transverse eigensolutions are sinusoids of the form $sin(n\pi x/w)$, and $k_V = 0$.

In order to apply the modal analysis technique to non-uniform quantum waveguides, the structure is first decomposed into junctions and uniform waveguide sections. Figure 1 illustrates an arbitrary junction which connects N quantum waveguides. Across the interfaces $\Delta S_i (i = 1, \ldots, N)$ between the uniform

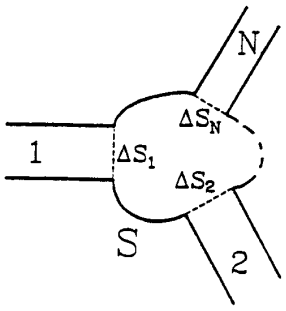

Figure 1: An arbitrary junction connecting N uniform quantum waveguide sections

waveguides and the discontinuity region, the continuity of the wave function and its normal derivative must be fulfilled. These continuity equations are solved for the scattering parameters by employing the mode-matching technique which requires the orthogonality of the eigensolutions ϕ_n in the uniform waveguides as well as in the discontinuity region. The requirement of orthogonal eigenfunctions in the discontinuity region, however, limits the applicability of the mode-matching technique to junctions for which such solutions are available.

As a result of the application of the mode-matching method, a generalized scattering matrix (GSM) is obtained which characterizes the junction [10]. It is evident that the GSM is of infinite order, and therefore it must be suitably truncated (which is equivalent to truncating the modal expansions) for numerical solutions. The analysis of a junction can be advantageously simplified by applying a decomposition method developed by Kühn [11] for the characterization of multiport metallic waveguide circuits. As illustrated in Fig. 2, the discontinuity region is decomposed into N open cavity regions. The solution of the wave function is obtained as a superposition of

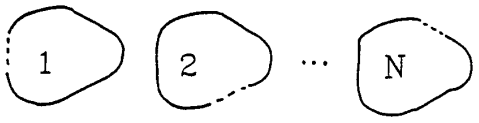

Figure 2: Decomposition of the junction discontinuity region

the partial wave solutions in each cavity. To obtain the generalized scattering parameters of a composite structure consisting of junctions and uniform waveguide sections, the individual GSMs are combined by employing an extension of the GSM technique [10] as described in Ref. [12]. The advantage of the extended GSM technique is that the number of modes that are coupled between adjacent junctions can be chosen independently from the number of modes retained in the calculation of the scattering parameters characterizing the junctions. From the transmission coefficient the two-terminal conductance of a nonuniform quantum waveguide structure in the limit of negligible bias voltage and zero temperature is computed as [13]-[17]

$$G = \frac{2e^2}{h} \sum_n T_n(E_f) \tag{4}$$

where $T_n(E_f)$ is the transmission coefficient from input mode n to all propagating modes at the output, evaluated at the Fermi energy. For the case of nonzero electron temperature, the conductance can be obtained from the zero-temperature conductance with the temperature-dependent Landauer-Büttiker formula [18] as

$$G(T) = -\int \frac{\partial f(E)}{\partial E} g(E, T = 0) dE \tag{5}$$

where $f(E)$ is taken as the Fermi-Dirac distribution function.

3 Convergence Properties

For the correct computation of the generalized scattering parameters of a quantum waveguide junction, it

must be understood how the truncation of the infinite wave function expansions influences the solution. In the GSM calculation for metallic step discontinuities, different converged results may be obtained for different ratios of modes retained on either side of the step discontinuity [19], [20]. This convergence problem, referred to as relative convergence, has been found to be related to the violation of the field distribution at the edge of metallic boundaries [19]. Theoretical studies have shown that the correct converged result is obtained if the ratio of modes on each side of the step is taken the same as the ratio of the corresponding waveguide widths.

The influence of the number of modes retained in the wave function expansions is illustrated in Fig. 3 for a step discontinuity in a quantum waveguide assuming

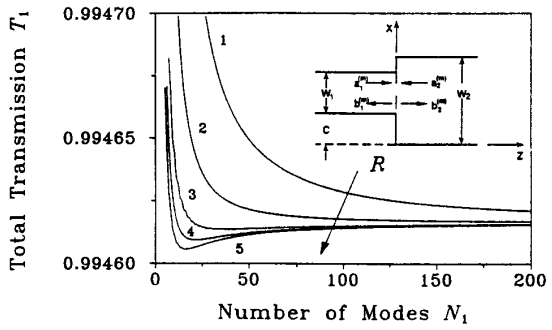

Figure 3: Convergence of T_1 through a step discontinuity shown in the inset with $w_1 = 10nm$, $w_2 = 20nm$, $c = 0$, $E = 100meV$. The ratio of modes retained on either side is defined as $R = N_2/N_1$.

hard wall boundaries, where the total transmission T_1 from the lowest mode to all propagating modes at the output is shown. A convergence to different end values for different mode ratios cannot be seen from this plot. However, it is found from Fig. 3 and further calculations not shown here that the fastest convergence is obtained for ratios in the number of modes on each side close to approximately 1.5 times the ratio of the corresponding widths. This result is similar to convergence investigations on planar waveguides [21] and coupled finlines [22]. To appreciate the improvement in the rate of convergence which may be obtained with the proper choice of the mode ratio, the following simple comparison is made. As seen in Fig. 3, 200 modes are needed with $R = 1$ to obtain a value with an absolute error of less than approximately 4.0×10^{-6}. Similarly, the necessary number of modes for a mode ratio of 1.5 times the width ratio giving the same maximum absolute error is 17 in the narrow guide and 51 in the wide guide, which corresponds to a reduction to less than 1% of the CPU time for the case with mode ratio $R = 1$.

4 Conductance Through Bend Discontinuities

It is well known from the study of electromagnetic waveguides that bend discontinuities give rise to scattering of incident waves which may exhibit resonance-like behavior. In quantum structures, experimental studies have been reported on double bend structures realized in split-gate high mobility heterojunction layers [23], [24]. In these studies, the double bend is realized by patterning the metal gate over a two-dimensional electron gas structure. When biased to depletion under the gates, a one dimensional channel is formed between the gates in which the double bend is defined. Figure 4 shows a schematic of an ideal dou-

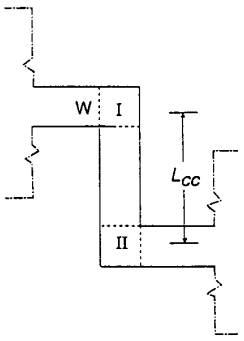

Figure 4: Schematic of an ideal double bend waveguide

ble bend quantum waveguide in which L_{cc} is the center to center distance between the uniform input waveguides to the bend. Figure 5 shows the measured conductance versus gate voltage from Ref. [24] at $50mK$ for the lowest plateau for two different values of L_{cc}. In the split-gate structure used, more negative gate bias pinches off the one-dimensional channel, effectively decreasing the width of the channel. As shown, a number of resonance peaks are evident, particularly in the longer bend compared with a nominal straight waveguide (shown in the inset).

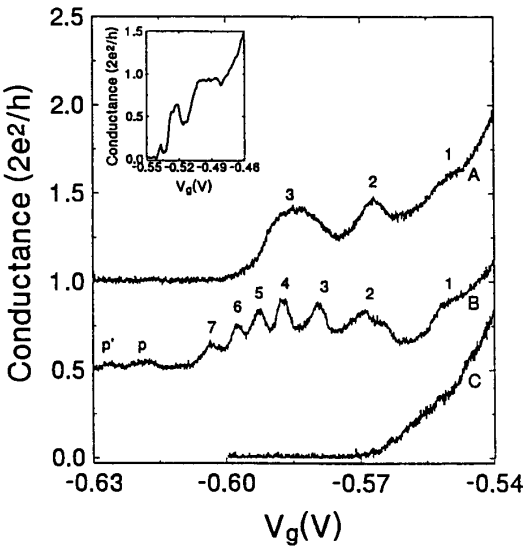

Figure 5: The experimental conductance versus gate bias of a double bend structure at $50mK$. Curves A and B are for $L_{cc} = 177$ and $293nm$, and are offset in conductance by $2e^2/h$ and e^2/h, respectively. The inset shows the conductance at $50mK$ of the device with $L_{cc} = 0$ (after Wu *et al.* [24])

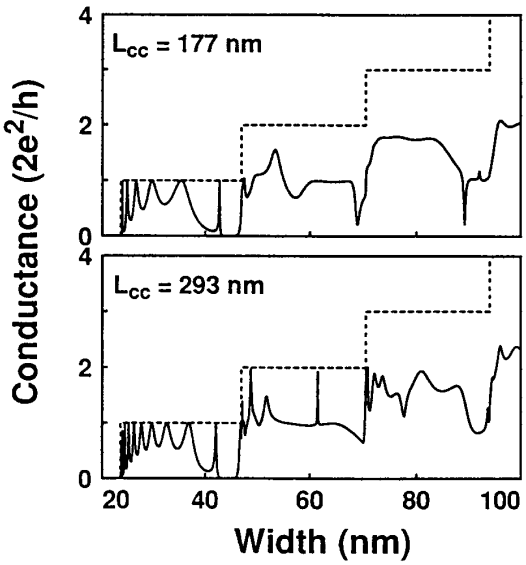

Figure 6: The computed conductance at $0K$ for two double-bend structures with $L_{cc} = 177$ and $293nm$. The dashed line shows the ideal behavior without the bends.

The modal analysis technique has been applied to study double bend structures [24] with different center-to-center lengths L_{cc} as defined in Fig. 4. Figure 6 shows the calculated zero-temperature conductance versus channel width (rather than gate voltage) of a double bend with $L_{cc} = 177nm$ and $L_{cc} = 293nm$, respectively, corresponding to the structures measured in Fig. 5. The electron density was taken as $2.85 \times 10^{11} cm^{-2}$ in both cases as was determined experimentally from magneto-transport measurements. Also included in the figures is the conductance in the absence of the bend discontinuities which, as expected, shows an ideal staircase behavior. The calculated conductance versus channel width for the double bend structures shows a strong resonance behavior in the first plateau. The region with zero conductance is due to a single right-angle bend as was shown previously [7], [12]. The resonance peaks in the conductance are caused by electron wave interference in the cavity region between the cascaded bends. A comparison of the calculated conductance for $L_{cc} = 177nm$ and $L_{cc} = 293nm$ (Fig. 6) shows an increased number of resonance peaks for the double-bend structure with the larger value of L_{cc}. This correlates qualitatively with the experimental data in Fig. 5.

The effect of a finite temperature on the conductance of a double-bend structure is demonstrated in Fig. 7. With increasing temperature, the sharper resonance peaks are washed out more rapidly than the broader peaks, effectively reducing the total number of resonance peaks in the lowest plateau. The conductance peaks are almost entirely eliminated for temperatures around $4.2K$. The finite temperature causes an averaging of the transmission coefficient over a narrow energy range around the Fermi level. This averaging may also represent the effect of non-ideal electron reservoirs where the electron energy is broadened around the Fermi level due to inhomogeneities [25].

Qualitatively, the calculated conductance versus gate voltage shows similar behavior to the experimental data. As is obvious, however, several notable differences appear. One is that the peak to valley ratio of the calculated resonance peaks is much larger than that measured experimentally. As seen in Fig. 7, one can partially account for this effect by assuming an effective temperature greater than the lattice temperature, although this is difficult to justify, even with impurity broadening for the high mobility samples stud-

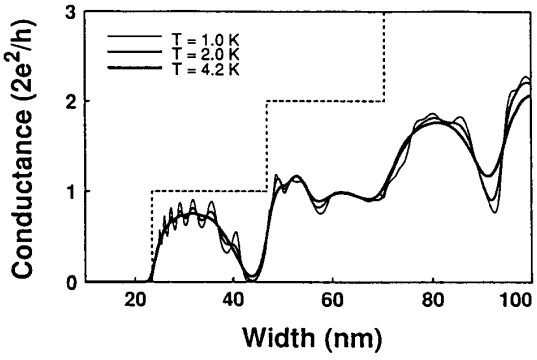

Figure 7: The calculated conductance for $L_{cc} = 293nm$ at finite temperature

ied experimentally. A more likely reason is that the right-angle bends shown in Fig. 4 are an idealization of the actual potential seen by electrons. Since the channel is defined electrostatically by reverse biased Schottky barriers, the actual bend potential experienced by the electrons is expected to be rounded as indicated by the inset of Fig. 8. There, semi-circular bends are shown, for which the conductance may be obtained by applying a mode-matching theory similar to that

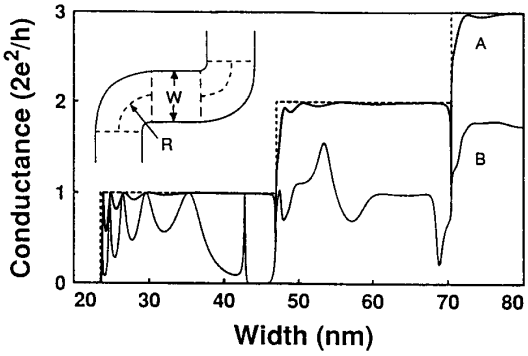

Figure 8: Calculated conductance for rounded versus square corners. Curve A is the conductance for semi-circular bens while curve B is the corresponding right-angle bend result for $L_{cc} = 177nm$. The inset shows a schematic of the double-bend with rounded corners.

for right-angle bends [26]. Fig. 8 shows a comparison of the conductance for a double-bend structure with rounded corners and right-angled corners. It can be seen that the position of the conductance resonances is nearly independent of the type of bend used. However, the peak-to-valley ratio of the resonances is noticeably reduced with rounded bends. In addition, the broad dip to zero conductance due to a single right-angle bend is not present for curved bends. The conductance of the actual experimental structure is expected to lie somewhere between the extreme cases of a right-angle bend and a curved bend with rounded corners shown in Fig. 8.

A further difference between the theoretical and experimental conductance is that the peak conductance experimentally is less than the plateau conductance, $2e^2/h$, whereas the peak theoretical conductance with or without rounding always approaches the quantized conductance limit. In order to explain this behavior, additional back-scattering must be present which reduces the ideal conductance below $2e^2/h$. One possible source of such scattering is boundary roughness due to irregular gate electrodes. Such irregularities are impossible to avoid using state of the art lithography techniques. The theoretical effect of boundary roughness in quantum waveguides has been reported elsewhere [27].

5 Lateral Transport Through Quantum Dots

Resonant tunneling through double barrier heterojunction structures has been studied now for a number of years [28], [29]. There negative differential resistance (NDR) is exhibited in the I-V characteristics when the Fermi level in the emitter is biased through the quasi-bound state(s) formed in the well between the two barriers. The same principle should be realizable in lateral double barrier structures fabricated in a similar fashion to the quantum waveguides discussed in Section 4 [30].

Figure 9 shows a schematic of a 'quantum dot' in which the shaded regions represent the gate electrode in a split-gate high electron mobility sample. The dot is defined by an input and output constriction which couple to external emitter and collector regions. We have previously modeled the transport properties of this system using the mode matching theory described in Section 2. To model the emitter and collectors, uniform waveguides are assumed in which the width is made sufficiently wide to not influence the conductance through the dot. It should be noted that the process of using wide input leads increases the numerical load by increasing the number of input modes which need to be retained in the mode-matching method, and thus there is an upper limit to the width which

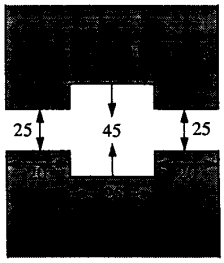

Figure 9: Quantum dot structure with input and output constrictions. Dimensions shown are in nanometers.

may be employed practically. Figure 10 shows the transmission coefficient as a function of energy in equilibrium for the curve labeled 0. The quantum dot dimensions have been chosen to correspond to typical dimensions that could be realized using electron

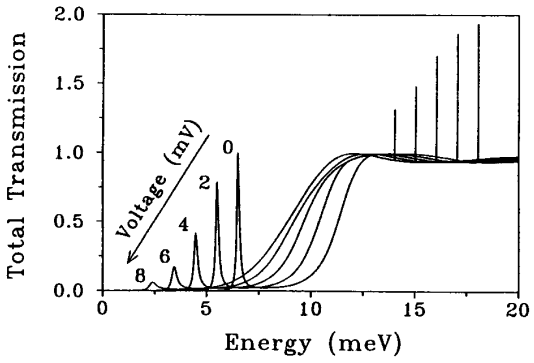

Figure 10: Total transmission as a function of energy for different emitter-collector bias voltages for the lateral quantum dot structure shown in Fig. 9 (after Weisshaar *et al.* [30])

beam lithography. The calculated transmission coefficient shows a strong resonance peak below the lowest conductance plateau associated with lateral tunneling through the quasi-bound state of the dot. Above this energy, the transmission approaches unity through the first mode. This unity transmission in turn gives rise to a plateau conductance of $2e^2/h$ in agreement with the experimental measurement of the non-addition of quantized ballistic conductance for phase coherent systems [31]. The calculated result agrees quite well with the measured conductance through the same split gate structure reported by Dzurak *et al.* [32].

As a bias is applied between the emitter and collector (left and right wide regions), the solution changes as potential is dropped across the structure. Here for simplicity, self-consistent effects associated with charge storage are neglected, and the applied voltage is assumed to drop linearly across the structure. The curves labeled other than 0 in Fig. 10 represent the transmission coefficient for the bias voltages shown. As is evident, the asymmetry in the barriers causes the resonance peak to diminish, while the transmission in the continuum continues to exhibit a unity value.

The corresponding current-voltage characteristics at various lattice temperatures are calculated using the finite temperature formula (5) as shown in Fig. 11. The I-V characteristics exhibit NDR for lattice tem-

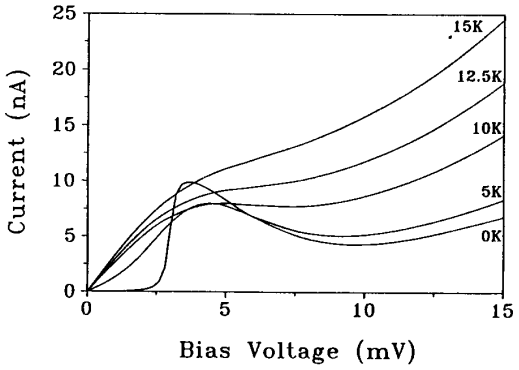

Figure 11: I-V characteristics at different temperatures for the double constriction structure shown in Fig. 9 (after Weisshaar *et al.* [30])

peratures up to $5K$, above which thermal broadening smears out the resonance sufficiently to eliminate the effect. If the structure in Fig. 9 is realized using metal gates above a two-dimensional electron gas, then the dimensions may be changed with gate bias, giving independent control of the NDR.

If transport through the quantum dot is not coherent, then the quantized conductance is reduced below the ideal $2e^2/h$ as was shown by Kouwenhoven *et al.* [33]. Recently, nonlinear transport through a quantum dot has been measured which shows strong instabilities in the I-V characteristics giving rise to S-type negative differential conductance (SNDC) [34]. This behavior cannot be explained by the coherent

transport mechanism discussed above in connection with lateral resonant tunneling. Rather, the explanation corresponds to the incoherent or sequential case which goes beyond the simple Landauer-Büttiker formalism [35]. In this explanation, electrons trapped in the quantum dot are driven out of equilibrium by the current passing through the dot. Energy is transferred to the dot electrons through e-e scattering which in turn raises the effective electron temperature there. Using a sequential tunneling model, and determining the electron temperature independently from energy balance considerations, the experimental bistability of the current-voltage characteristics may be reproduced theoretically as shown in Fig. 12. There the theoretical and experimental I-V characteristics are shown for two different gate biases on the contacts forming

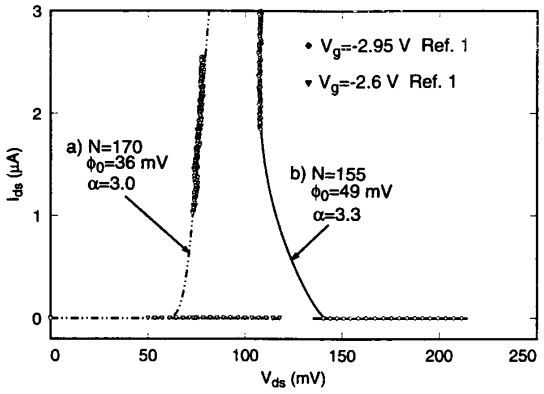

Figure 12: Calculated and experimental current voltage characteristics through a quantum dot structure exhibiting SNDC for two different gate biases (after Goodnick *et al.* [35])

the dot (somewhat similar to that shown in Fig. 9). The fit parameters shown correspond to the number of electrons in the dot, N, the potential barrier in the constrictions to electrons entering the dot, ϕ_0, and a parameter characterizing the reduction in barrier with potential drop across the constriction. The electron temperature in the dot is near the lattice temperature in the high impedance regime, but rises quickly to several hundred Kelvin in the low impedance state.

Acknowledgements

The authors would like to acknowledge the support of the Office of Naval Research.

References

[1] F. Sols, M. Marcucci, U. Ravaioli, and K. Hess, "Theory for a quantum modulated transistor," *J. Appl. Phys.*, Vol. 66, pp. 3892-3906, 1989.

[2] E. G. Haanappel and D. van der Marel, "Conductance oscillations in two-dimensional Sharvin point contacts," *Phys. Rev. B*, Vol. 39, pp. 5484-5487, 1989.

[3] H. U. Baranger, "Multiprobe electron waveguides: filtering and bend resistances," *Phys. Rev. B*, Vol. 42, pp. 11479-11495, 1990.

[4] A. Szafer and A. D. Stone, "Theory of quantum conduction through a constriction," *Phys. Rev. Lett.*, Vol. 62, pp. 300-303, 1989.

[5] E. Tekman and S. Ciraci, "Novel features of quantum conduction in a constriction," *Phys. Rev. B*, Vol. 39, pp. 8772-8775, 1989.

[6] G. Kirczenow, "Theory of the conductance of ballistic quantum channels," *Solid State Comm.*, Vol. 68, pp. 715-718, 1988.

[7] A. Weisshaar, J. Lary, S. M. Goodnick, and V. K. Tripathi, "Analysis of discontinuities in quantum waveguide structures," *Appl. Phys. Lett.*, Vol. 55, pp. 2114-2116, 1989.

[8] C. S. Lent and D. J. Kirkner, "The quantum transmitting boundary method," *J. Appl. Phys.*, Vol. 67, pp. 6353-6359, 1990.

[9] A. Weisshaar, S. M. Goodnick, and V. K. Tripathi, "Modal Analysis Applied to Quantum Waveguide Structures and Discontinuities," *Superlatt. Microstruct.*, Vol. 12, pp. 37-41, 1992.

[10] T. Itoh, Ed. *Numerical Techniques for Microwave and Millimeter-Wave Passive Structures*, Wiley, 1989.

[11] E. Kühn, "A mode-matching method for solving field problems in waveguide and resonator circuits," *Arch. Elek. Übertragung.*, Vol. 27, pp. 511-513, 1973.

[12] A. Weisshaar, J. Lary, S. M. Goodnick, and V. K. Tripathi, "Analysis and Modeling of Quantum Waveguide Structures and Devices," *J. Appl. Phys.*, Vol. 70, pp. 355-366, 1991.

[13] R. Landauer, "Electrical resistance of disordered one-dimensional lattices," *Philos. Mag.*, Vol. 21, pp. 863-867, 1970.

[14] P. W. Anderson, D. J. Thouless, E. Abrahams, and D. S. Fisher, "New method for a scaling theory of localization," *Phys. Rev. B*, Vol. 22, pp. 3519-3526, 1980.

[15] D. S. Fisher and P. A. Lee, "Relationship between conductivity and transmission matrix," *Phys. Rev. B*, Vol. 23, pp. 6851-6854, 1981.

[16] M. Büttiker, "Role of quantum coherence in series resistors," *Phys. Rev. B*, Vol. 33, pp. 3020-3026, 1986.

[17] Y. Imry, in *Directions in Condensed Matter Physics*, edited by G. Grinstein and G. Mazenko, World Scientific, Singapore, Vol. 1, pp. 101-163, 1986.

[18] S. Datta, "Quantum Devices," *Superlatt. Microstruct. 6*, Vol. 6, pp. 83-93, 1989.

[19] R. Mittra and S. W. Lee, *Analytical Techniques in the Theory of Guided Waves*, MacMillan, New York, 1971.

[20] Y. C. Shih, in em Numerical Techniques for Microwave and Millimeter-Wave Passive Structures, edited by T. Itoh, Wiley, New York, 1989.

[21] H. Hofmann, "Dispersion of planar waveguides for millimeter-wave application," *Arch. Elek. Übertragung.*, Vol. 31, pp. 40-44, 1977.

[22] G. Schiavon, R. Sorrentino, and P. Tognolatt, "Characterization of coupled finlines by generalized transverse resonance method," *Int. J. Numer. Model.*, Vol. 1, pp. 45-59, 1988.

[23] J.C. Wu, M.N. Wybourne, W. Yindeepol, A. Weisshaar, and S.M. Goodnick, "Interference phenomena due to a double bend in a quantum wire," *Appl. Phys. Lett.*, Vol. 59, pp. 102-104, 1991.

[24] J.C. Wu, M.N. Wybourne, A. Weisshaar, and S.M. Goodnick, "Waveguide effects in quantum wires with double-bend discontinuities," *J. Appl. Phys.*, Vol. 74, pp. 4590-4597, 1993.

[25] S. Das Sarma and B. Vinter, "Effect of impurity scattering on the distribution function in two-dimensional Fermi systems," *Phys. Rev. B*, Vol. 24, pp. 549-553, 1981.

[26] A. Weisshaar, S. M. Goodnick, and V. K. Tripathi, "A rigorous and efficient method of moments solution for curved waveguide bends," *IEEE Trans. Microwave Theory Tech.*, Vol. 40, pp. 2200-2206, 1992.

[27] Y. Takagaki and D.K. Ferry, "Conductance of quantum waveguides with a rough boundary," *J. Phys.: Cond. Matter*, Vol. 4, pp. 10421-10432, 1992.

[28] T.C.L.G. Sollner, W.D. Goodhue, P.E. Tannenwald, C.D. Parker, and D.D. Peck, "Resonant tunneling through quantum wells at frequencies up to $1.5THz$," *Appl. Phys. Lett.*, Vol. 43, pp. 588-590, 1983.

[29] F. Capasso, K. Mohammed, and A.Y. Cho, "Resonant tunneling through double barriers, perpendicular quantum transport in superlattices, and their device applications," *IEEE J. Quantum Electron.*, Vol. QE-22, pp. 1853-1869, 1986.

[30] A. Weisshaar, J. Lary, S.M. Goodnick, and V.K. Tripathi, "Negative differential resistance in a resonant quantum wire structure," *IEEE Elec. Dev. Lett.*, Vol. 12, pp. 2-4, 1991.

[31] D.A. Wharam, M. Pepper, H. Ahmed, J.E.F. Frost, D.G. hasko, D.C. Peacock, D.A. Ritchie, and G.A.C. Jones, "Addition of the one-dimensional quantised ballistic resistance", *J. Phys. C*, Vol. 21, pp. L887-L891, 1988.

[32] A.S. Dzurak, M. Field, J.E.F. Frost, I.M. Castleton, C.G. Smith, C.-T. Liang, M. Pepper, D.A. Ritchie, E.He. Linfield, and G.A.C. Jones, "Conductance in quantum boxes: interference and single electron effects," to be published, proceedings of the NATO ASI on Quantum Transport in Ultra Small Devices, Il Ciocco, Italy, July, 1994.

[33] L.P. Kouwenhoven, B.M. van Wees, W. Kool, C.J.P.M. Harmans, A.A.M. Staring, and C.T. Foxon, "Transition from Ohmic to adiabatic transport in quantum point contacts in series," *Phys. Rev. B*, Vol. 40, pp. 8083-8086, 1989.

[34] J.C. Wu, M.N. Wybourne, C. Berven, S.M. Goodnick, and D.D. Smith, "Negative differential conductance observed in a lateral double constriction device," *Appl. Phys. Lett.*, Vol. 61, pp. 2425-2427, 1992.

[35] S.M. Goodnick, J.C. Wu, M.N. Wybourne, and D.D. Smith, "Hot-electron bistability in quantum-dot structures," *Phys. Rev. B*, Vol. 48, pp. 9150-9153, 1993.